PERGAMON

Renewable Energy 23 (2001) 621–639

RENEWABLE ENERGY

www.elsevier.nl/locate/renene

Study of the solar radiation over Menia

M.A. Mosalam Shaltout *, A.H. Hassan, A.M. Fathy

National Research Institute of Astronomy and Geophysics, Helwan, Cairo, Egypt

Abstract

Measurements were carried out at El-Menia (28.12°N, 30.55°E) in Egypt, which lies in the middle of Egypt, 244 km south of Cairo, for a complete year (1997). Measurements were taken using the Eppley pyranometer to measure the global solar radiation (*G*) in the range from 280 to 2800 nm, and the Eppley pyrheliometer, which measures the normal incidence solar radiation (*I*) in the range from 280 to 2800 mn along with four direct spectral bands measured using three cutoff Schott glass filters in the range B1 (280–530 mn), B2 (530–630 nm), B3 (630–695 nm) and B4 (695–2800 nm). The monthly variations for all the parameters and the correlations between the different parameters have been calculated. The diffuse solar radiation and the diffuse fraction for Menia have been calculated using three different methods. Computation of the atmospheric turbidity coefficient for each spectral band was carried out using two methods, the Linke and Angstrom methods. The Linke turbidity factor is between 2.01 and 5.86, while the Angstrom turbidity coefficient is between 0.09 and 0.223. This last result shows that Menia is considered to be a highly polluted region.

1. Introduction

The data used in this paper are from a single year measured from January 1997 to December 1997, as hourly values from 8:00 to 16:00 for the global solar radiation (*G*) and the normal incidence solar radiation (*I*) beside four direct spectral bands (B1, B2, B3 and B4). There are some meteorological parameters measured in parallel with the radiation components, such as the air temperature (*T*), relative humidity (RH) and visibility (*V*). The data were measured on the roof of the Physics Department, Faculty of Science, Menia University. Menia is a polluted city, where pollution is due to the dust from the eastern desert and water vapor from plants and water

* Corresponding author. Tel.: +2-010-5156-443; fax: +2-02-556-8020.
E-mail address: mamshaltout@frcu.eun.eg (M.A. Mosalam Shaltout).

0960-1481/01/$ - see front matter
PII: S0960-1481(00)00136-1

sources in Menia which make the atmosphere unstable. Pollution also arises from the Cairo–Aswan highway which is crowded with traffic and leads to a large amount of smoke in the atmosphere at Menia University that absorbs the global solar radiation [1].

Determination of the turbidity of the atmosphere is becoming increasingly important because it integrates the total loading of aerosol in the atmosphere. Atmospheric turbidity is generally recognized as the extinction of solar radiation by suspended particles with radii from 0.1 to 10 μm. Total or spectral measurements of the intensity of direct solar radiation are frequently used to calculate a turbidity index. Each index is referred to the extinction at a specific wavelength or spectral interval [2]. For the separation of the radiant energy from a source such as the sun into reasonably well-defined bands, filters are more practical and easier to handle than a spectrophotometer. With carefully calibrated filters, measuring is as easy as the more normal pyrheliometric observation of the total solar intensity. One of the difficulties of comparing filtered radiation data assembled at different places is that the transmission of the filters employed can show small variations for a supposedly standard filter glass, from melt to melt and even within the same melt. One method for measuring atmospheric turbidity is the pyrheliometric method. This method consists of measuring the solar intensity through broad-band filters. These are short-wave cutoff glass filters which transmit solar radiation of wavelengths greater than 530 nm (Schott RG1), 630 nm (Schott RG2), and 695 nm (RG8). The measured intensity through the filters is normally used to compute the turbidity with the methods described by Linke and Boda in 1922, Angstrom in 1929 and Schüepp in 1949. More detailed information is given in the IGY Instruction Manual and the guide to Meteorological Instruction and Observing Practices. The evaluation of broad-band filter data requires assumptions about the wavelength dependence of the aerosol extinction coefficient. Extraterrestrial solar spectral irradiance data are needed. These data are at the present time only available with an absolute accuracy of 2%. Consequently, the accuracy of turbidity determinations is uncertain [3].

2. Hourly mean variation of solar radiation components

2.1. Global solar radiation (G)

Fig. 1 shows the monthly variation of global solar radiation as hourly values, where each set of 3 months represents a particular season, and we find the highest global solar radiation values lie in the summer months (June, July and August), while the lowest values lie in the winter months (December, January and February) and the global solar radiation values are seen to be equal through the autumn and spring months.

The before-noon hours from 8:00 to 11:00 are lower than the after-noon hours from 13:00 to 16:00 becuase of the intensive water vapor due to the evaporation of water from the Nile River and El-Ebrahimia Canal, where they lie to the east of the

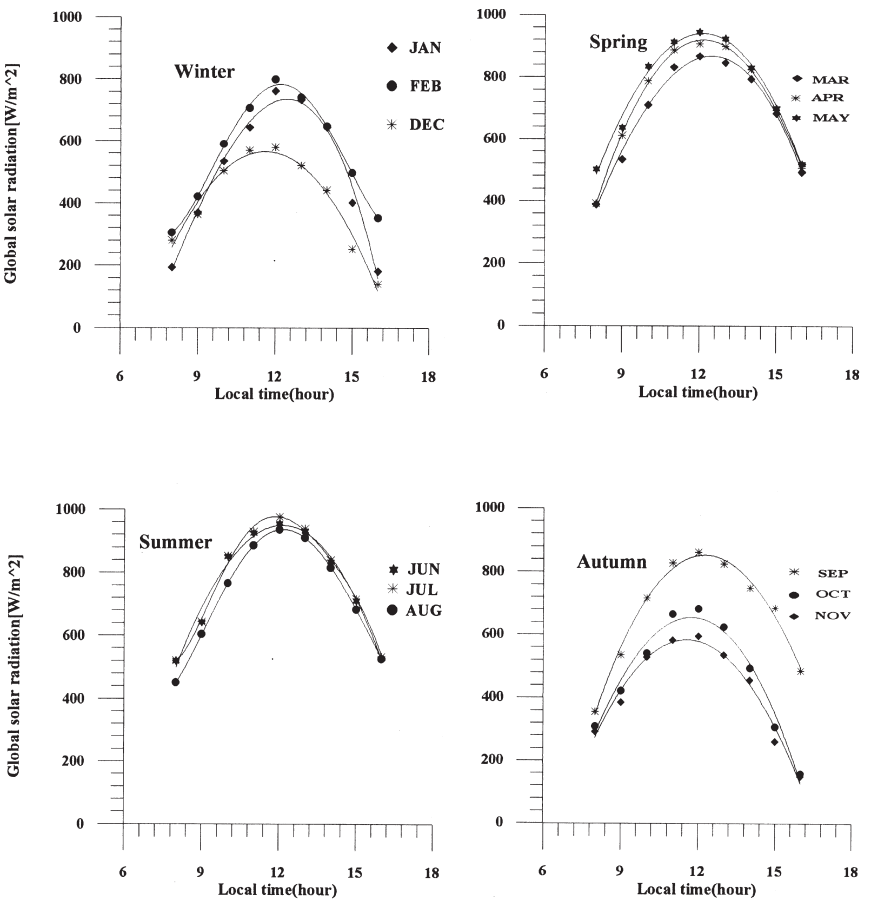

Fig. 1. Monthly variation of global solar radiation as hourly values for Menia city in W/m^2.

measuring place, next to some factories which produce pollutant materials in the Menia atmosphere in this direction.

The intensity values of G for the summer months are close together (June and July) as shown in Fig. 1, where the intensity value of June is 765 W/m^2 while it is 771 W/m^2 in July. The winter months are divergent (February and December), where the intensity value for February is 561 W/m^2 while that for December is 404 W/m^2. The highest intensity value is in summer, with a mean value of 755 W/m^2, while the lowest intensity value is in winter, with a mean value of 487 W/m^2.

2.2. Direct total solar radiation (I)

Direct total solar radiation (I) is the white solar radiation band which covers the wavelength 280–2800 nm.

Fig. 2 shows the monthly variation for I as hourly values where the highest intensity value lies in the winter and spring months around noon (from 11:00 to 13:00), while the values in the summer months are higher than the values in the other months for the remaining daytime hours.

The differences between the monthly values of I for each season are different as shown in Fig. 2, where we find the summer months are close together (June and July), where the intensity value of June is 782 W/m^2 while it is 786 W/m^2 in July. Winter months have a large difference between them, where the intensity value for December is 633 W/m^2, while the intensity value for February is 824 W/m^2.

From Fig. 2, we notice that the direct total solar radiation is fast increasing through the winter months for the before-noon hours and fast decreasing for the after-noon hours due to the large change in the air mass from hour to hour, while for the summer months the change is slowly increasing and slowly decreasing before and after noon, where noon is at 12:00. As an example of this, note that the intensity value of I for

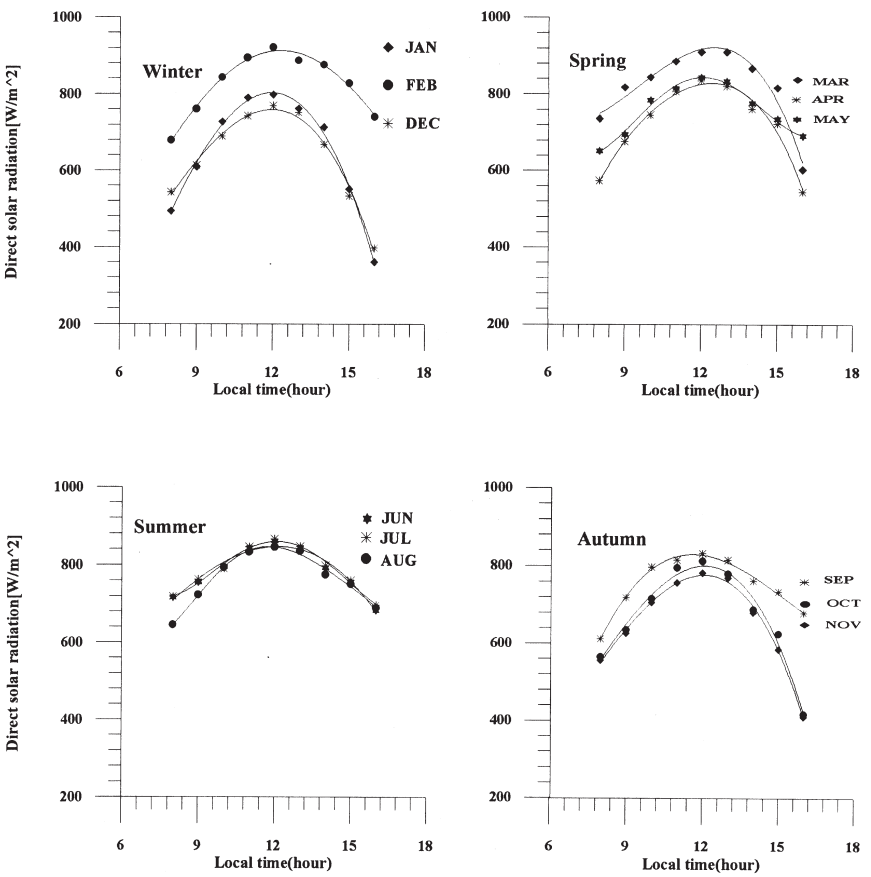

Fig. 2. Monthly variation of direct solar radiation as hourly values in the spectral band 280–2800 nm in W/m^2.

January at noon is 797 W/m^2, while the value 4 h later is 36O W/m^2 and 4 h earlier the value is 493 W/m^2, where the air mass at noon is 1.5, while 4 h later it is 3.85 and 4 h earlier it is 4.5. The opposite results are seen for the summer months such as July, where the intensity value at noon is 872 W/m^2, while 4 h later it is 697 W/m^2 and 4 h before it is 718 W/m^2, where the air mass at noon is 1.007, while 4 h later it is 1.69 and 4 h earlier it is 1.74. From the last results we conclude that the important factor that affects the solar radiation is the air mass, which is equal to sec(θ), where θ is the solar zenith angle.

The decreasing values in the summer months around the noon hour are due to the high amount of water vapor and the high air pollution value in the sky through these hours which change the color of the sky from blue to white, where the milky pollution through these hours in the summer is coming from the eastern desert which has a very high amount of dust. The highest intensity value is in summer with a value of 778 W/m^2, while the lowest value is in autumn with a value of 691 W/m^2.

2.3. Direct solar radiation spectral bands

In our study we have four direct spectral bands measured using three cutoff Schott glass filters in the range B1 (280–530 nm), B2 (530–630 nm), B3 (630–695 nm) and B4 (695–2800 nm) shown in Fig. 3. The first band represents the violet+blue

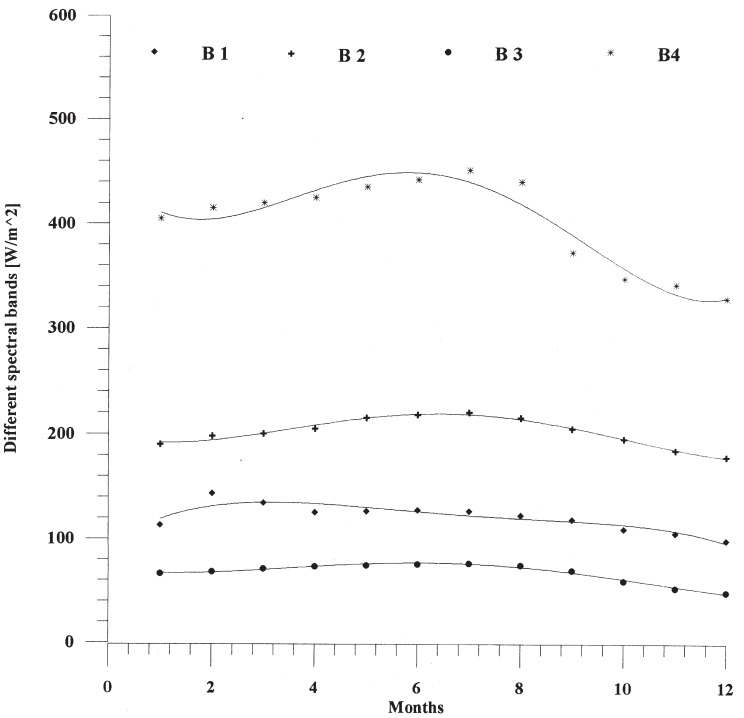

Fig. 3. Monthly mean variation of different solar radiation spectral bands at noon in W/m^2.

colors and is B1 (280–530 nm), where the highest values for this band lie in February with mean intensity value (mean of 9 h) of 200 W/m^2, while the lowest value is in December with a value of 142 W/m^2. The highest intensity B1 value is in the summer season with a value (mean of 9 h) of 183 W/m^2, while the lowest value is in the autumn with a value of 161 W/m^2.

The second band represents the yellow+green colors and is B2 (530–630 nm), where the highest intensity values lie in March with a value (mean of 9 h) of 124 W/m^2, while the lowest value is in December with a value of 76 W/m^2. The highest intensity B2 value is in the spring season with a value (mean of 9 h) of 115 W/m^2, while the lowest value is in the autumn with a value of 92 W/m^2.

The third band represents the red color and is B3 (630–695 nm), where the highest intensity values lie in March with a value (mean of 9 h) of 71 W/m^2, while the lowest value is in December with a value of 40 W/m^2. The highest intensity B3 value is in the spring season with a value of 66 W/m^2, while the lowest value is in the autumn with a value of 48 W/m^2.

The fourth band represents infra-red color and is B4 (695–2800 nm), where the highest intensity values lie in March with a value (mean of 9 h) of 438 W/m^2, while the lowest value is in December with a value of 286 W/m^2. The highest intensity B4 value is in the summer and the spring seasons with a value (mean of 9 h) of 413 W/m^2, while the lowest value is in the autumn with a value of 320 W/m^2.

Fig. 3 shows the four spectral bands for the direct solar radiation, B1, B2, B3 and B4, where B4 has the biggest annual mean value which is 375 W/m^2, while for B1 the annual mean value is 173 W/m^2, for B2 it is 104 W/m^2 and for B3 it is 58 W/m^2. The value of B4/I is 51%, B1/I is 24%, while B2/I is 16% and B3/I is 9%, where the highest percentage is in B4 and the lowest in B3. These results are different from those given in [1, 4] for Helwan where it is 58% for B4, and 19.77% for B1, while it is 13.2% for B2 and for B3 8.52%. The differences between Menia and the work at Helwan arise because for Menia the data are a mean over 9 h, while for Helwan the data are measured from sunrise to sunset and also there is high pollution in Helwan.

Generally, we conclude that for the four bands the highest values are in the winter and spring months through the noon hours while the highest values for all other daytime hours lie in the summer months, and the lowest values are in the autumn months due to the high variation in the air mass from winter to summer.

The solar radiation components are affected by the presence of the intensive water vapor content in the Menia sky through the summer and spring seasons and also through autumn but with a lower amount, and finally through the winter the effect of water vapor content disappears from the Menia sky. The high amount of water vapor through the summer and spring seasons in the Menia sky is due to the high temperature which leads to evaporated water vapor from the Nile River and from El-Ebrahimia canal to the east of Menia University where the measurements were taken.

Table 1
Relations between B1, B2, B3, B4 and G against I

Equations	CC%	RMS
$\log(B1)=1.02\times\log(I)-1.62$	82	1.82
$\log(B2)=0.89\times\log(I)-1.23$	82	1.45
$\log(B3)=1.16\times\log(I)-3.59$	81	2.65
$\log(B4)=0.8\times\log(I)+0.64$	83	1.06
$\log(G)=2.15\times\log(I)-7.8$	91	3.35

3. Relations between the different spectral bands against the total direct solar radiation (I)

The relation between the different spectral bands against I is very important because sometimes we need a certain band, where we can't measure it. The relations given here between the different spectral bands and the global solar radiation against the total direct solar radiation are produced using the first order power equation which is:

$$\log(y)=a\times\log(x)+b \tag{1}$$

The relations between B1, B2, B3, B4 and G against I are given in Table 1. The relations between the spectral bands B1 and B2 against the direct solar radiation I are high with correlation coefficients of 82% for both relations, while against B3 the correlation coefficient is 81%, and it is 83% for B4.

Finally, the relation between the global solar radiation and the direct solar radiation is very high with a correlation coefficient of 91%. From the last relations we conclude that by increasing any spectral band the direct solar radiation will be increased in parallel.

Now we shall study the relations between the clearness index for each band against the total clearness index $Kt(G/G_0)$. The special equations for these relations are given in Table 2. We find a very high correlation coefficient between each band's clearness index and Kt, where there are very high correlation coefficients between $K1$(B1/B01),

Table 2
Relations between Kt against $K1$, $K2$, $K3$ and $K4$

Equations	CC%	RMS
$\log(K1)=1.02\times\log(Kt)+0.13$	95	0.005
$\log(K2)=0.58\times\log(Kt)+0.36$	96	0.01
$\log(K3)=2.49\times\log(Kt)+0.79$	90	0.07
$\log(K4)=2.2\times\log(Kt)-0.59$	89	0.06
$\log(KI)=0.99\times\log(Kt)-1.14$	95	0.005

*K*2(B2/B02) and *KI*(*I*/*I*0) against *Kt*, where the correlation coefficients for them are 95%.

The relation between *K*3(B3/B03) and *K*4(B4/B04) against *Kt* is also very high with correlation coefficients of 90%.

The relations between the meteorological parameters (*T* and RH) and the solar radiation components (*G*, *I*, B1, B2, B3 and B4) are given in Table 3, where we find good correlation coefficients between *G*, *I*, B2, B3 and B4 against the ambient temperature *T*, and a very good correlation coefficient between B1 against *T*. The correlation coefficients between *G*, B1, B3 and B4 against relative humidity RH are high, while the correlation coefficients between *I* and B2 against RH are very high as given in Table 3.

4. Atmospheric turbidity

4.1. Angstrom turbidity

The scattering causes a certain degree of extinction of incoming light, characterized by an extinction function which can be expressed as:

$$f(\lambda)=\beta\lambda^{-\alpha} \tag{2}$$

where λ denotes the wavelength of the incoming light; β denotes the extinction coefficient at $\lambda=10^3$ nm, and α denotes a factor (wavelength exponent) related to the size distribution of the particles responsible for the extinction=1.3 suggested by Angstrom [5] and it varies between 0 and 4.

The IGY Instruction Manual recommends the calculation of β using the RG630 filter and the clear filter measurements (250–630 nm). The turbidity of the atmos-

Table 3
Relations between *G*, *I*, B1, B2, B3 and B4 against *T* and RH for Menia

Temperature in °C W/m²	Equations	CC%	RMS
G	$T=0.02\times G+11.8$	64	14.1
I	$T=0.08\times I-36$	64	14
B1	$T=0.28\times B1-27$	82	7.8
B2	$T=0.3\times B2-6.6$	61	14.8
B3	$T=0.28\times B3+10$	57	15.9
B4	$T=0.05\times B4+9.3$	46	18
Relative humidity (%)			
G	$RH=-0.05\times G+84.4$	88	14.5
I	$RH=-0.2\times I+20$	91	11.1
B1	$RH=-0.47\times B1+14$	84	19.2
B2	$RH=-0.75\times B2+13.3$	91	11.3
B3	$RH=-0.7\times B3+9.2$	85	18.7
B4	$RH=-0.14\times B4+9.9$	77	26.7

phere is defined as the reduced transparency of the atmosphere, caused by absorption and scattering of radiation by solid or liquid particles, other than clouds, held in suspension. As developed by Angstrom, the turbidity of the atmosphere is defined by β, the extinction coefficient at $\lambda=10^3$ nm, normally called the turbidity coefficient, and α, the wavelength exponent. β values less than 0.10 normally denote a very clear condition whereas values greater than 0.20 are a distinctly hazy condition.

The extinction due to water vapor absorption can be ignored if the calculations are made only for those wavelength intervals $\lambda<700$ nm. The instrument used was an Epply pyrheliometr equipped with Schott filters OG530, RG630 and RG695. Their main characteristics (lower cutoff wavelength, and correction factor CF) are given in Table 4. A quartz filter was also used with a nominal cutoff wavelength of approximately 2800 nm. The average value of α, which is dependent on the particle size distribution, was found by Angstrom to be about 1.3. The distribution of the size of the suspended particles greater than approximately 100 nm is governed by the formula:

$$dN=kr^{-\gamma}\,dr \tag{3}$$

where r is the particle radius, dN is the number of particles per unit volume in the size range r to $r+dr$, k is a constant dependent on the total number of particles and, γ is an exponent which determines the "slope" of the particle number versus size curve. In practice r varies from about 3 to 5 as a typical value for polluted atmospheres and a typical value for a clean atmosphere is 4.

These values were obtained by solving the Bouguer equation:

$$I_{\Delta\lambda}=I_{0\Delta\lambda}\exp[-m(\tau_{R\Delta\lambda}+\tau_{z\Delta\lambda}+\beta\lambda^{-\alpha}) \tag{4}$$

so that

$$\beta=\frac{1}{m}\lambda^{-\alpha}[\ln(I_{0\Delta\lambda}/I_{\Delta\lambda})-M(\tau_{R\Delta\lambda}+\tau_{z\Delta\lambda})] \tag{5}$$

where $I_{0\Delta\lambda}$ denotes the spectral irradiance observed outside the atmosphere at the mean sun–earth distance in the wavelength band (spectral interval) $\Delta\lambda$, $I_{\Delta\lambda}$ denotes the spectral irradiance observed at the instrument in the same spectral interval, $\tau_{R\Delta\lambda}$ denotes the average extinction coefficient over the wavelength interval for molecules (Rayleigh scattering), $\tau_{z\Delta\lambda}$ denotes the average extinction coefficient over the wavelength interval for ozone and M denotes the air mass.

A simple expression by Kasten for the air mass that we use for all solar zenith angles is:

Table 4
Values of λ_m and CF of the filters [2]

Filter	OG530	RG630	RG695
λ_m (nm)	530	630	695
CF	1.082	1.068	1.042

$$M=[\cos\theta+0.15(93.885-\theta)^{-1.253}]^{-1} \quad (6)$$

where θ denotes the solar zenith angle.

The pyrheliometer technique developed by Schüepp in 1949 requires replacing $\beta\lambda^{-\alpha}$ in Eq. (4) with B and using logarithms to the base 10 rather e. The same assumptions used in the determination of β apply to the determination of B with the exception that Schüepp calculated the wavelength exponent α. This was done by calculating B values for two wavelengths intervals $530<\lambda<630$ nm and $630<\lambda<695$ nm with this information:

$$\alpha=[\ln(B_1/B_2)/\ln(\lambda_2/\lambda_1)] \quad (7)$$

A turbidity coefficient value for 500 nm can then be calculated:

$$\ln B_{500\ \mathrm{nm}}=\alpha[\ln(\lambda_2/500)]+\ln B_{\lambda 2} \quad (8)$$

Since the mean values of the two wavelength intervals cited above are relatively close together, i.e. $\lambda_1\approx590$ nm and $\lambda_2\approx660$ nm, small errors in the computed B1 and B2 values can result in large variations in α. It is recommended that if all three filters are used, α should be determined from either of the band pairs listed below:

1. I=$280<\lambda<2800$ nm
2. B1=$280<\lambda<530$ nm
3. B2=$530<\lambda<630$ nm
4. B3=$630<\lambda<695$ nm
5. B4=$695<\lambda<2800$ nm

Since the average attenuation in the broad band intervals changes with air mass, the average wavelength for these intervals will also change. One method of selecting the average wavelength is to assign it that wavelength for which the average attenuation $(\tau_R+\tau_z)M$, has the same values as the $(\tau_R+\tau_z)$ value for M=1. For the broad-band intervals ($\lambda<500$ nm, $\lambda<630$ nm, $\lambda<695$ nm), the average Rayleigh and ozone attenuation is a function of the air mass [6]. These variation are given in Table 5.

Table 5
The average Rayleigh and ozone attenuation functions in air mass (m) [7]

Band	$\Delta\lambda$	$(\bar{\tau}_R+\bar{\tau}_z)$		$\bar{\lambda}$		$I_{0\Delta\lambda}$ cal cm^{-2} min^{-1}
		m=1	m=5	m=1	m=5	
B9	$250<\lambda<530$ nm	0.164	0.117	396	430	0.558
B6	$530<\lambda<630$ nm	0.051		591		0.270
B7	$630<\lambda<695$ nm	0.028		662		0.150

Using the appropriate values for $(\tau_R+\tau_z)$ and $I_{0\Delta\lambda}$, B may be calculated for any spectral intervals from the following relationship:

$$B=\frac{\ln\dfrac{Io\Delta\lambda}{I\Delta\lambda}s}{M\ln 10}-(\bar{\tau}_R+\bar{\tau}_z) \tag{9}$$

The factor s in the equation is used to adjust the observed irradiance to the mean sun–earth distance. Angstrom in 1929 determined that α has an average value of 1.3 when the wavelength is given in microns, so that

$$B=1.069\beta \tag{10}$$

In practice, α varies between about 0 and 4 depending on the particle size distribution, so the exact relationship between β and B requires an accurate knowledge of the wavelength exponent. In addition, determinations of β are generally made from pyrheliometer measurements of the radiation in relatively broad spectral intervals [8].

4.2. Linke turbidity

For cloudless skies, water vapor and aerosol content are the two main factors producing significant variations in the Helwan solar radiation climate. Assumed fixed concentrations of the absorbing gases describes the method for calculating the direct irradiance normal to the solar beam as a function of optical air mass, perceptible water, and a turbidity coefficient L. L is defined as the additional attenuation at unit air mass of the solar beam due to the presence of aerosol in the atmosphere. The equation for the determination of $I(I)$ is:

$$I=RI_0\exp(-Lm)\ \mathrm{W/m^2} \tag{11}$$

The Linke turbidity factor is estimated from the expression according to [9]:

$$L=P(m)[\log I_0-\log I-2\log R] \tag{12}$$

where $P(m)$ is a function of the air mass m and R is the earth–sun distance in astronomical units. The values of $P(m)$ which are used in this study are obtained by the next formula which is the best fit of the values given by Coulson:

$$P(m)=22.64m^{-0.801}\ \text{for}1\leq m\leq 4 \tag{12a}$$

Ayinlis and Rattunde [10], proposed a classification of various sites in terms of atmospheric clearness using the following criteria related to the Atmospheric Transparency Index (ATT) as shown in Table 6.

Table 6
Classification of various sites in terms of atmospheric clearness [10][a]

Atmospheric transparency index (ATI)	Turbidity type	Class of turbidity
>0.79	Very clear atmosphere	1
0.76–0.79	Clear atmosphere	2
0.72–0.76	Urban atmosphere	3
<0.72	Industrial atmosphere	4

[a] ATI=0.820+0.00193φ−0.036L, φ is the latitude, the angular location north or south of the equator, north positive; $-90° \leq \phi \leq 90°$.

5. Hourly mean variation of Linke turbidity factor

Linke turbidity for Menia is affected by the high dust and pollution in the summer months and by the high water vapor content in the atmosphere or the high relative humidity through the winter months. For Menia, we have special characteristics where turbidity is affected by pollution from industry and from Menia airport and also from the eastern desert which is considered the main source of dust in the Menia atmosphere. Linke was the first to suggest that the quantity L would be reasonably independent of the air mass or at least less dependent on m than the extinction coefficient for a turbid atmosphere. This has in fact proved to be correct and L has been employed as a useful measure of atmospheric turbidity. It is clear from Eqs. (9) and (10) that L can never be less than unity. Thus it is easy to appreciate that a turbidity factor of 1.5 represents a rather clear atmosphere, while a turbidity factor of say 5 refers to turbid air, while its value can vary from 1 to 10 [11].

Table 7 gives the seasonal variation of the Linke turbidity factor (L) for the different spectral bands where for the direct solar radiation (I) the range of the Linke turbidity factor is from 2.95 to 5.26.

The maximum value for $L(I)$ is in the summer months due to the high dust and pollution, while the minimum is in winter due to the high dew droplets which particulate the dust and the pollution. The highest value for $L(I)$ is in April due to the high dust concentration caused by the occurrence of Khamssin depressions. The minimum value for $L(I)$ is in March, as characterized by a clean atmosphere (especially after the passage of a cold front). March can be considered as a transitional month from the winter regime (extratropical depressions) to the spring regime (Khamssin depressions). There are also minimum values in October, November and December due to the inversion of weather conditions coming from the Mediterranean sea. The highest $L(I)$ is in summer with a value of 4.89 (turbid), while the lowest value is in winter with a value of 3.34 (turbid). We find the same characteristic for I in the different spectral bands B1, B2, B3 and B4. For the band B1 the range of L(B1) is from 2.01 to 4.55. The highest value is in summer with a value of 3.99 (turbid), while the lowest value is in winter with a value of 2.73 (turbid). For the band B2 the range of L(B2) is from 2.58 to 5.14. The highest value is in autumn with a value of 4.31 (turbid), while the lowest value is in winter with a value of 3.24 (turbid).

Table 7
Seasonal mean variation for Linke turbidity factor as hourly values for the different direct spectral bands

	L[*I*]				*L*[B1]			
Hour	Winter	Spring	Summer	Autumn	Winter	Spring	Summer	Autumn
8	3.01	4.23	4.45	3.99	3.07	4.38	4.49	4.14
9	3.35	4.43	4.87	4.43	3.35	4.28	4.42	4.40
10	3.48	4.63	5.02	4.42	3.10	3.78	3.85	3.63
11	3.51	4.65	5.11	4.50	2.53	3.26	3.57	3.44
12	3.59	4.80	5.26	4.61	2.01	2.99	3.42	3.21
13	3.55	4.60	5.11	4.35	2.53	2.78	3.68	3.77
14	3.40	4.38	5.00	4.21	2.85	3.47	3.76	3.58
15	3.18	4.26	4.74	4.12	2.45	3.63	4.20	3.77
16	2.95	4.08	4.51	3.96	2.69	3.62	4.55	3.14
Mean	3.34	4.45	4.89	4.29	2.73	3.58	3.99	3.68
Hour	*L*[B2]				*L*[B3]			
8	2.93	4.18	4.05	4.66	2.82	3.58	3.85	4.96
9	3.73	3.75	4.11	5.14	3.63	3.78	4.46	5.73
10	3.44	3.79	4.22	4.98	3.39	3.88	4.55	5.76
11	3.33	3.55	4.19	4.61	3.55	3.90	4.39	5.81
12	3.07	3.30	4.01	3.96	3.43	3.08	3.81	4.69
13	3.41	3.27	4.06	4.20	3.76	3.21	4.53	5.55
14	3.47	3.31	4.05	4.23	3.51	3.57	4.12	5.21
15	3.20	3.01	3.82	3.86	3.81	3.32	4.48	4.99
16	2.58	3.32	3.66	3.16	3.19	3.55	4.13	4.09
Mean	3.24	3.50	4.02	4.31	3.45	3.54	4.28	5.20
Hour	*L*[B4]							
8	2.58	3.74	3.82	4.37				
9	3.24	4.42	4.38	5.17				
10	3.60	4.29	4.60	5.52				
11	3.74	4.21	4.61	5.54				
12	3.85	4.01	4.53	5.53				
13	3.80	3.92	5.00	5.44				
14	3.70	4.08	4.78	5.27				
15	3.86	4.07	4.48	4.91				
16	2.93	4.12	3.99	3.32				
Mean	3.48	4.07	4.47	5.01				

For the band B3 the range of *L*(B3) is from 2.82 to 5.81, with the highest value in autumn with a value of 5.2 (turbid), while the lowest value is in winter with a value of 3.45 (turbid). For the band B4 the range of *L*(B4) is from 2.58 to 5.54. The highest value is in autumn with a value of 5.01 (turbid), while the lowest value is in winter with a value of 3.48 (turbid). Finally, from the last results for the Linke turbidity factor we classify Menia as a *turbid atmospheric region*.

6. Hourly mean variation of Angstrom turbidity coefficient

The Angstrom turbidity coefficient for Menia is affected by the high air temperature in the summer months and by the high water vapor content in the atmosphere or the high relative humidity through the winter months. It is also affected by the pollution from the industry and from the eastern desert for Menia which is considered the main source of dust in the Menia atmosphere.

The Angstrom turbidity coefficient (β) is currently determine from measurements of the direct beam of solar radiation (I). Its value varies typically from 0.0 to 0.5. Iqbal [12] shows parameters for various degrees of atmospheric cleanliness as a clean atmosphere has β equal to 0.0, a clear atmosphere has β as 0.1, and a turbid atmosphere has β as 0.2 while a very turbid atmosphere has β as 0.4.

Table 8 gives the seasonal variation of the Angstrom turbidity coefficient (β) for the different spectral bands where for the direct solar radiation (I) the range of $\beta(I)$ is from 0.1 to 0.18 (turbid). The maximum value for $\beta(I)$ is in the spring months due to the high dust and pollution. The highest value of $\beta(I)$ is in spring with a value of 0.167 (turbid), while the lowest value is in winter with a value of 0.138 (turbid).

For the band B1 the range of β(B1) is from 0.093 to 0.176 (turbid). The highest value of β(B1) is in autumn with a value of 0.140 (turbid), while the lowest value is in winter with a value of 0.113 (turbid). For the band B2 the range of β(B2) is from 0.093 to 0.193. The highest value of β(B2) is in autumn with a value of 0.164 (turbid), while the lowest value is in winter with a value of 0.131 (turbid).

For the band B3 the range of β(B3) is from 0.1 to 0.23. The highest value of β(B3) is in autumn with a value of 0.197 (turbid), while the lowest value is in spring with a value of 0.131 (turbid). For the band B4 the range of β(B4) is from 0.09 to 0.223. The highest value of β(B4) is in autumn with a value of 0.191 (turbid), while the lowest value is in winter with a value of 0.141 (turbid).

Finally, from the last results for the Angstrom turbidity coefficient we classify Menia as a *turbid atmospheric region*.

7. Diffuse solar radiation and diffuse fraction

The diffuse solar radiation (D) can be calculated from the theoretical method from the following equations:

$$D_{\mathrm{h}} = G - I\cos\theta \tag{13}$$

and the total diffuse day is:

$$D = \int_{sR}^{ss} (G - I\cos\theta)\mathrm{d}h \tag{14}$$

The diffuse ratio or the diffuse fraction (Kd) can be calculated by two methods

Table 8
Seasonal hourly mean variation of Angstrom turbidity coefficient for different bands as hourly values

	$\beta[I]$				β[B1]			
Hour	Winter	Spring	Summer	Autumn	Winter	Spring	Summer	Autumn
8	0.100	0.150	0.143	0.143	0.110	0.153	0.147	0.143
9	0.133	0.177	0.167	0.173	0.127	0.160	0.150	0.167
10	0.147	0.180	0.173	0.177	0.130	0.143	0.130	0.147
11	0.147	0.177	0.163	0.173	0.117	0.123	0.120	0.140
12	0.150	0.167	0.180	0.167	0.093	0.117	0.113	0.127
13	0.153	0.160	0.177	0.163	0.117	0.110	0.123	0.150
14	0.150	0.173	0.170	0.160	0.123	0.133	0.127	0.137
15	0.147	0.160	0.163	0.157	0.100	0.137	0.143	0.140
16	0.117	0.160	0.147	0.127	0.097	0.133	0.150	0.107
Mean	0.138	0.167	0.165	0.160	0.113	0.134	0.134	0.140
	β[B2]				β[B3]			
8	0.103	0.147	0.130	0.163	0.100	0.120	0.123	0.170
9	0.147	0.140	0.137	0.190	0.140	0.137	0.150	0.220
10	0.143	0.143	0.143	0.193	0.147	0.150	0.157	0.230
11	0.147	0.137	0.147	0.187	0.147	0.150	0.150	0.230
12	0.127	0.130	0.133	0.160	0.147	0.120	0.127	0.190
13	0.147	0.127	0.143	0.170	0.163	0.123	0.160	0.217
14	0.147	0.127	0.137	0.163	0.147	0.140	0.140	0.200
15	0.127	0.110	0.127	0.140	0.143	0.117	0.153	0.183
16	0.093	0.117	0.120	0.107	0.110	0.123	0.140	0.137
Mean	0.131	0.131	0.135	0.164	0.138	0.131	0.144	0.197
	β[B4]							
8	0.090	0.133	0.123	0.157				
9	0.127	0.160	0.147	0.193				
10	0.150	0.167	0.160	0.220				
11	0.163	0.167	0.160	0.220				
12	0.170	0.157	0.160	0.223				
13	0.163	0.153	0.177	0.217				
14	0.153	0.157	0.167	0.203				
15	0.150	0.153	0.153	0.180				
16	0.103	0.147	0.127	0.110				
Mean	0.141	0.155	0.153	0.191				

according to three methods which are Collares (Kd_C), Page (Kd_P) and the theoretical method.

The first equation calculates the daily diffuse components of solar irradiance depending on clearness indexes (Kt) is given by Collares [13] as following:

$$Kd_C = D/G = a - bc \tag{15}$$

where a=0.775+0.00606(H_s−90), b=0.505+0.00456(H_s−90), c=cos (115Kt−103), H_s=cos^{-1} [−tan φtan δ], Kt=G/Go.

The value of Kd lies between zero and unity, depending on atmospheric conditions; Kd approaches unity under heavily overcast conditions.

Also, the diffuse fraction can be calculated by the Page equation [14] as follows:

$$Kd_P = 1 - 1.13Kt \tag{16}$$

And finally Kd can be calculated according to the theoretical method as:

$$Kd = D/G \tag{17}$$

We can also compute the diffuse solar radiation from Kd as follows:

$$D = G \times Kd \ (Kd_P \text{ and } Kd_C) \tag{18}$$

7.1. Computation for the diffuse solar fraction over Menia

The monthly variation values for Kd_C, Kd_P and Kd_t are given in Table 9 where Kd_P values are higher than Kd_C and Kd_t values for all months except January, also Kd_t values are higher than Kd_C values for all months. For the monthly variation of the Kd values, the mean value of Kd_C ranged from 0.16 to 0.22, while for Kd_P it ranged from 0.11 to 0.36 and for Kd_t it ranged from 0.17 to 0.4. The seasonal variation of the diffuse fraction is given from Table 9, where the highest value of Kd_P is in autumn, while the lowest is in spring. The highest Kd_C and Kd_t values are in winter, while the lowest values are in summer.

The diffuse solar radiation (D) can be calculated from the diffuse fraction (Kd) according to Eq. (13). The value of Kd can be calculated by two methods according to Eqs. (15) and (16) for Collares (Kd_C) and Page (Kd_P), respectively.

The monthly variations of the diffuse solar radiation computed by three methods at noon are shown in Fig. 4. The D_P values for Menia are higher than the values for D_C and D_t through all months, while the D_C and D_t nearly have the same value. The highest D_P value (mean of 9 h) is in June with an intensity value of 177 W/m^2, where the lowest value is in December with a value of 129 W/m^2, while the highest value for D_C is in June with a value of 138 W/m^2 and the lowest value is in December with a value of 93 W/m^2. The highest value of D_t is in June with a value of 137 W/m^2 while the lowest value is in December with a value of 88 W/m^2.

Finally, we notice that the values for D_C and D_t are nearly the same, while there are big differences between them and D_P which is 38 W/m^2 (31% of D_t or D_C). This result shows that the best methods with which to calculate the diffuse solar radiation in Menia are Collares and the theoretical method.

Table 9
Seasonal variation of diffuse fraction *Kd* (Kd_P, Kd_C and Kd_t) computed by three methods for Menia

	[*KdP*]				[*KdC*]			
Hour	Winter	Spring	Summer	Autumn	Winter	Spring	Summer	Autumn
8	0.176	0.290	0.258	0.355	0.244	0.202	0.199	0.209
9	0.275	0.275	0.278	0.369	0.217	0.166	0.169	0.180
10	0.223	0.210	0.199	0.310	0.205	0.166	0.158	0.168
11	0.206	0.193	0.189	0.275	0.195	0.150	0.138	0.162
12	0.157	0.192	0.176	0.266	0.195	0.142	0.126	0.161
13	0.187	0.181	0.178	0.282	0.195	0.154	0.140	0.166
14	0.194	0.168	0.194	0.292	0.205	0.174	0.159	0.181
15	0.320	0.150	0.197	0.345	0.210	0.197	0.182	0.195
16	0.369	0.155	0.215	0.357	0.231	0.218	0.204	0.223
Mean	0.234	0.202	0.209	0.317	0.211	0.176	0.164	0.183

	[Kdt]			
	Winter	Spring	Summer	Autumn
8	0.436	0.232	0.204	0.256
9	0.266	0.163	0.119	0.142
10	0.221	0.166	0.127	0.117
11	0.182	0.136	0.092	0.105
12	0.204	0.101	0.140	0.088
13	0.201	0.110	0.138	0.075
14	0.242	0.167	0.142	0.134
15	0.244	0.250	0.195	0.189
16	0.380	0.392	0.252	0.335
Mean	0.264	0.191	0.157	0.160

8. Conclusions

1. For global solar radiation *G*, the highest *G* values are in summer with a mean value (mean of 9 h) of 755 W/m^2, while the lowest intensity value is in winter with a mean value of 487 W/m^2. The before-noon hours from 8:00–11:00 are lower than the after-noon hours from 13:00–16:00 due to the intensive water vapor caused by the evaporation of the water from the Nile River and El-Ebrahimia canal where they lie to the east of the measuring place. The intensity values for the summer months are close together which is the same result for the spring months, while the winter months are divergent, where the intensity value for February is 561 W/m^2, while for December it is 404 W/m^2.
2. For direct solar radiation *I*, the highest intensity value is in summer with a value (mean of 9 h) of 778 W/m^2, while the lowest value is in autumn with a value of 691 W/m^2. The highest intensity value of *I* at noon is in July with a value of 872 W/m^2, while the lowest value is in December with a value of 760 W/m^2.
3. For the spectral bands, the highest value of B1 at noon is in July with a value

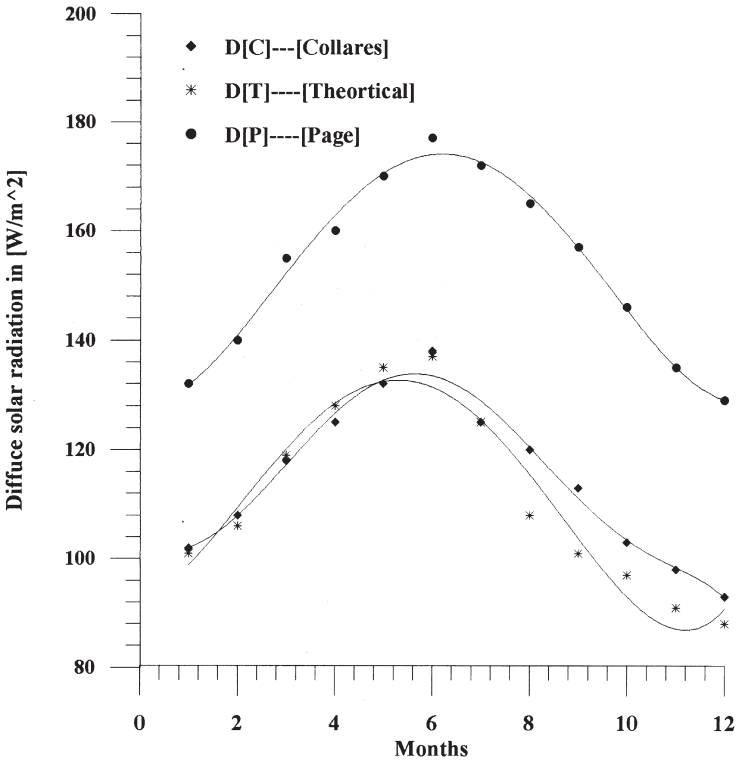

Fig. 4. Diffuse solar radiation calculated by three different methods for Menia at noon in W/m^2.

of 220 W/m^2, while the lowest value is in December with a value of 178 W/m^2. The highest value for B2 at noon is in July with a value of 127 W/m^2, while the lowest value is in December with a value of 98 W/m^2. Finally, the highest value for B3 is in July with a value of 76 W/m^2 while the lowest value is in December with a value of 48 W/m^2, and also the highest value for B4 is in July with a value of 451 W/m^2, while the lowest value is in December with a value of 328 W/m^2. The four bands have their highest values in the winter and the spring months through the noon hours while the highest values for all other daytime hours lie in the summer months and the lowest values are in the autumn months due to the high variation of the air mass from winter to summer.

4. The relations between the different spectral bands against I have high correlation coefficients. We also find a good correlation between T and RH and the solar radiation components.
5. The relations between the clearness index for each band against the total clearness index Kt are very high relations that have very high correlation coefficients.
6. For the Linke turbidity factor L, the value (mean of 9 h) for $L(I)$ is from 2.95 to 5.26, where the highest value is in the summer months, while the minimum value is in the winter. The range for L(B1) is from 2.01 to 4.55, while it is from 2.58

to 5.14 for L(B2). Also L(B3) has values ranged from 2.82 to 5.81 and finally for L(B4) values ranged from 2.85 to 5.54.

7. For the Angstrom turbidity coefficient β, $\beta(I)$ values (mean of 9 h) ranged from 0.1 to 0.0.18, where the maximum is in the summer months, while the minimum value is in the winter months. For β(B1) values it ranged from 0.093 to 0.176, while for β(B2) it is from 0.093 to 0.193. Also for β(B3) it ranged from 0.1 to 0.23, while β(B4) is from 0.09 to 0.223.
8. For Menia data, the diffuse solar radiation D, the D_P values for Menia are higher than the values for D_C and D_t through all months, while the D_C and D_t have nearly the same value. The annual average value for Kd_P is higher than the annual average value for Kd_C by 24%, while it is higher than Kd_t by 20%. The annual average value for Kd_t is higher than the annual average value for Kd_C by 5%. Therefore, the best international model is the Collares model.

References

[1] Mosalam Shaltout MA. Egyptian Solar Radiation Atlas. Cairo, Egypt: USAID, 1991.
[2] Annual Report of WMO—International operations handbook for measurement of background atmospheric pollution, No.491, 1978.
[3] Bird RE et al. Solar spectral measurements in the terrestrial environment. Appl Optics 1982;21(8):223–7.
[4] Fathy AM. Ultraviolet solar radiation at Helwan and its dependence on atmospheric conditions. MSc Thesis, Helwan University, 125 pp, 1992.
[5] Prescott JA. Evaporation from a water surface in relation to solar radiation. Trans R Soc S Austr 1940;64:114–8.
[6] Garge HP. Treatise. On solar energy. Wiley-Interscience Publication, 1982.
[7] Annual Report WMO—Operations manual for sampling and analysis techniques for chemical constituents in air and precipitation, No. 299. Geneva, Switzerland: WMO, 1974.
[8] Gruter W et al. Solar radiation data from satellite images. D. Reidel Publishing Company, 1986.
[9] Pinazo JM et al. A new method to determine Angstrom's turbidity coefficient, its application for Valencia. Solar Energy 1995;54(4):219–26.
[10] Aydinlis X, Rattunde R. Final report on calculation methods for the radiation data on inclined surfaces and calculated atlas data. In: EEC Solar Energy Program—Project F—Action 3.2, September, 1982:22–32.
[11] Robinson N. Solar radiation. New York: Elsevier Publishing Company, 1966.
[12] Iqbal M. An introduction to solar radiation. Canada: Academic Press, 1983.
[13] Collares M, Pereeiraa, Radl AA. The average distribution of solar radiation correlations between diffuse and hemispherical and between daily and hourly insolation values. Solar Energy 1979;22(2):155–64.
[14] Liu BYH, Jordan. The interrelationship and characteristic distribution of direct, diffuse, and total solar radiation. Solar Energy 1960;4(3):1–19.